Proceedings of the 9th International Conference on Fluid Flow, Heat and Mass Transfer (FFHMT'22)
Niagara Falls, Canada – June 08-10, 2022
Paper No. 135
DOI: 10.11159/ffhmt22.135

Thermal Efficiency Improvement of Brayton Cycle in the Presence of Phase Change Material

Alireza Khademi[1], Seyed Ali Abtahi Mehrjardi[2], Saeed Tiari[3], Karim Mazaheri[2], Mohammad Behshad Shafii[1]
[1]Department of Mechanical Engineering, Sharif University of Technology
Azadi Ave, Tehran, Iran
alireza.khademi@alum.sharif.edu; behshad@sharif.edu
[2]Department of Aerospace Engineering, Sharif University of Technology
Azadi Ave, Tehran, Iran
seyedali.abtahimehrjardi@ae.sharif.edu; mazaheri@sharif.ir
[3]Department of Biomedical, Industrial and Systems Engineering, Gannon University
109 University Square, Erie, PA 16541, United States
tiari001@gannon.edu

Abstract – The objective of the present study was to improve the thermal efficiency of a Brayton cycle benefiting from the multiphase concepts of phase change in thermodynamics and incorporating it with a phase change material (PCM) melting system. This system could be alternatively used to decrease the temperature of intake air into the gas turbine and improve gas turbine efficiency. The present study investigated the presence of phase-change refrigeration storage. The complex system was modelled by a straightforward configuration of a rectangular cavity, which contained the phase change material with intermediate fluid. Reducing the temperature of the inlet air had a considerable impact on improving the thermal efficiency of the gas turbine cycles. In this study, a new cooling approach was proposed in which the intake air was cooled using a PCM-based heat exchanger along with an intake line. During the daylight hours, air moved over the phase change material, whose melting point was lower than the maximum temperature of the surrounding air. The melting process caused a decrease in surrounding air temperature before entering the compressor. Upon completion of the PCM melting, the necessary ambient air was taken from the surroundings utilizing conventional air inlet configurations. During the night-time, the ambient air was cooler, and the liquid PCM solidified. The temperature of the chosen PCM was lower than the maximum value of surrounding temperature. The numerical modelling of the PCM indicated that it was possible to reduce the temperature of the inlet air. The thermodynamic investigation of the results demonstrated that both the thermal efficiency and the power output increased at a specific surrounding temperature.

Keywords: Brayton cycle, Intake air cooling, Phase change material (PCM), Thermal efficiency, Melting process.

Nomenclature

C_p	specific heat (kJ/kg.K)
g	gravity (m/s^2)
ΔH	instant latent heat (kJ/kg)
k	thermal conductivity (W/m.K)
P	pressure (Pa)
Q	heat (J/s)
T	Temperature (°C)
t	time (s)
u	horizontal velocity component (m/s)
v	vertical velocity component (m/s)
W	power (J/s)

Greek Symbols

α	void fraction
β	thermal expansion (1/K)
Γ	mass flux (kg/m^2.s)
γ	liquid fraction
η	efficiency
μ	dynamic viscosity (kg/m.s)
ρ	density (kg/m^3)
Subscripts	
C	compressor
k	phase indicator
m	melting point
N	net
PCM	phase change material
T	turbine

1. Introduction

Power plant gas turbines operating with open cycles are engines with sensitivity to ambient temperature variations. Increasing the inlet air temperature, particularly noticeable in summer, significantly reduces the gas turbine output power. The inlet air temperature can be lowered using air cooling via water atomization or by mounting a chiller in the inlet ducting. Installing a cooler or chiller for intake air before entering the compressor to achieve a higher efficiency, is not economically reasonable. Moreover, they may be incompatible with weather conditions. A variety of air coolers were previously employed to examine the possible improvement of the electric output with chilling the turbine inlet air [1-3].

The customary solution is to directly apply mechanical refrigeration with a compression cooling device for cooling the air. This system offers the main drawback for electricity consumption at times of lesser turbine capacity, that is, during the warmest daytime when the activity, and therefore the electric demands, usually approach their maximum value (on-peak hours), considered as a parasitic power. A solution can be to employ chilling storage as the energy supply, and electricity consumption will be variable regardless of the time [4].

A study by Kakaras [5] indicated that the gas turbine output and effectiveness strongly depended on the ambient air temperature. According to the gas turbine type, power output was reduced by a proportion between 5% and 10% of the ISO-rated power output (15°C) for every 10 K rise of ambient air temperature.

Mohanty [6] observed that increasing the inlet air temperature from the ISO-rated condition to 30°C could reduce the net power output by 10%. Such a drop in the power output could be even higher for gas turbines with lower capacities. Besides, increasing the ambient temperature by 1°C led to a 1% reduction of the gas turbine rated capacity.

According to Ameri [7], decreasing the ambient temperature from 34.2°C to ISO-rated condition in a 16.6 MW gas turbine, could cause a 11.3% increase in the mean power output. It was further found that the power output would reduce by 0.74% for every 1°C rise of ambient air temperature.

A study on gas turbine plants at two locations in Oman, by Dawoud [8], reported the association of fogging cooling with 11.4% greater electrical energy compared with evaporative cooling in both zones. However, absorption cooling provided 40% and 55% higher energy than fogging cooling.

Alhazmy [1] presented evidence of a 0.57% mean power output elevation per 1°C reduction in inlet temperature. The power output rose by 10% during cold moist conditions, and by 18% during hot moist conditions.

A combined cycle power plant operating in Bangkok was investigated by Boonnasa [9], and the results revealed improved annual power output of the gas turbine by 10.6% and the combined cycle power plant by 6.24% as a result of falling temperature from 35°C to ISO-rated condition. The rating of the gas turbine was 110.76 MW.

In the present study, the rectangular storage represented the phase change material (PCM), and water was heated from the side wall imposing a constant heat flux boundary condition. The water was on top of the PCM. Hence, when the melting process started, the displacement of water and melted PCM during melting (water was denser than PCM), improved the melting process. Using PCM-water combination system at the compressor entrance in the Brayton cycle to reduce inlet air temperature has not been reported in previous studies.

2. Physical Model

The physical configuration was a 2D melting process of a solid PCM from the vertical wall of a rectangular enclosure. Figure 1 shows a schematic view of the configuration. When PCM was melted, the air that was in contact with PCM through the cavity, entered the compressor through a lower temperature cavity. The air entered the compressor from the cavity that ambient air crossed.

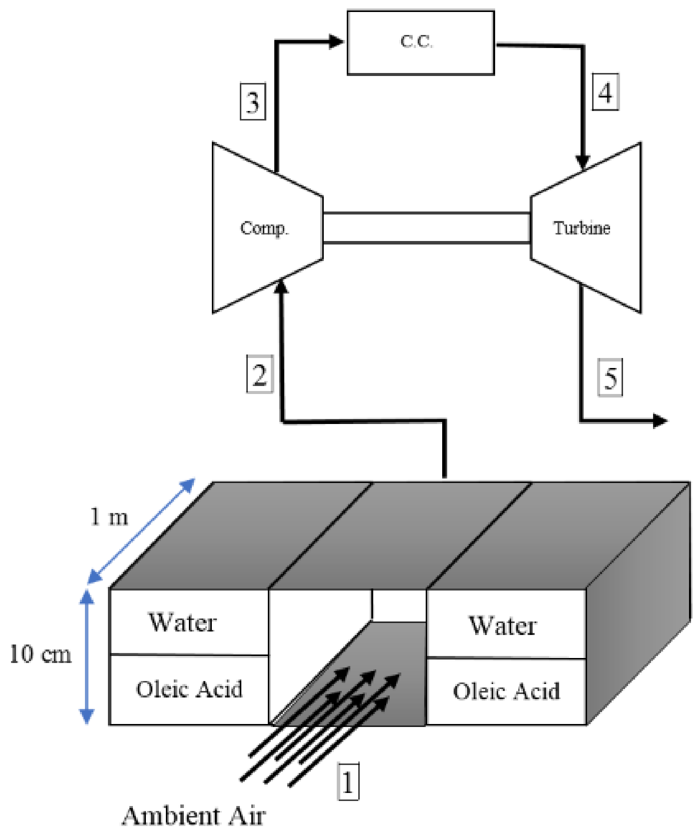

Fig. 1: Schematic configuration of system.

3. Thermodynamic Analysis of Brayton Cycle

The following equations define the net power output and thermal efficiency of the Brayton cycle [10]:

$$W_N = W_T + W_C - W_{PCM} \tag{1}$$

$$W_N = \eta(\dot{m}_a + \dot{m}_f)C_{p,mix}(T_4 - T_5) \tag{2}$$

$$W_T = \dot{m}_a C_{p,air}(T_3 - T_2) \tag{3}$$

$$Q_{heat\ exchanger} = \dot{m}_a C_{p,air}(T_1 - T_2) \tag{4}$$

4. Numerical Modeling

In this section, the governing equations will be discussed, the physical properties of the PCM and the numerical solution method.

4.1 Mathematical Formulation

The liquid PCM was assumed to be Newtonian and incompressible. Boussinesq approximation with constant thermo-physical features for each solid and liquid state (Table 1), was used to model volumetric changes during melting. The enthalpy-porosity method was employed to model the melting procedure [11]. This approach considered the entire computational dominion as a porous site, where the value of liquid fraction (γ, in the range of 0-1) represented the porosity. Taking the previous presumptions into consideration, the governing equations involving continuity, momentum, and energy equations include the following [12].

Continuity:

$$\frac{\partial(\alpha_k \rho_k)}{\partial t} + \frac{\partial(\alpha_k \rho_k u_k)}{\partial x} + \frac{\partial(\alpha_k \rho_k v_k)}{\partial y} = \Gamma_k \tag{5}$$

where,

$$\alpha_k = \frac{V_k}{V_{total}} \tag{6}$$

and,

$$\sum_{k=1}^{2} \Gamma_k = 0 \tag{7}$$

x-momentum:

$$\frac{\partial(\rho u)}{\partial t} + \frac{\partial(\rho uu)}{\partial x} + \frac{\partial(\rho uv)}{\partial y} = -\frac{\partial P}{\partial x} + \frac{\partial}{\partial x}\left(\mu \frac{\partial u}{\partial x}\right) + \frac{\partial}{\partial y}\left(\mu \frac{\partial u}{\partial y}\right) + Au \tag{8}$$

y-momentum:

$$\frac{\partial(\rho v)}{\partial t} + \frac{\partial(\rho uv)}{\partial x} + \frac{\partial(\rho vv)}{\partial y} = -\frac{\partial P}{\partial y} + \frac{\partial}{\partial x}\left(\mu \frac{\partial v}{\partial x}\right) + \frac{\partial}{\partial y}\left(\mu \frac{\partial v}{\partial y}\right) + Av + \rho g \beta (T - T_m) \tag{9}$$

energy:

$$\frac{\partial(\rho C_P T)}{\partial t} + \frac{\partial(\rho u C_P T)}{\partial x} + \frac{\partial(\rho v C_P T)}{\partial y} = +\frac{\partial}{\partial x}\left(k \frac{\partial T}{\partial x}\right) + \frac{\partial}{\partial y}\left(k \frac{\partial T}{\partial y}\right) - S \tag{10}$$

where,

$$S = \frac{\partial(\rho \Delta H)}{\partial t} + \frac{\partial(\rho u \Delta H)}{\partial x} + \frac{\partial(\rho v \Delta H)}{\partial y} \tag{11}$$

$$A = -C \frac{(1-\gamma)^2}{\gamma^3 + \varepsilon} \tag{12}$$

where ε is a small constant used to avoid division by zero and C is a constant, which reflects the morphology of the melting front. In this study, the values of ε and C were set equal to 10^{-6} and 10^{-3}, respectively.

Table 1: Thermo-physical properties of oleic acid (OA) and water [13-16].

Parameter	Value (OA)	Value (Water)
Specific heat (kJ/kg.K)	2.15	4.182
Melting temperature range (°C)	13-14	---
Latent heat of fusion (kJ/kg)	80.6	---
Thermal conductivity (W/m.K)	0.24	0.6
Density (kg/m3)	850	998.2

4.2 Numerical Validation

The validation was performed by comparing the melting fraction from the model to those of the numerical simulation of [17].

4.3 Boundary Conditions

The no-slip boundary condition was enforced on the walls. Also, the inner vertical wall had constant heat flux, and the other walls were insulated.

4.4 Numerical Simulation

The governing equations subject to the boundary and initial conditions were solved numerically by a control volume approach employing a uniform mesh. The spatial discretization of the differential equations necessarily included the second-order central difference approximation for the whole diffusion terms and the first order upwind approximation for the convective terms. The coupling between pressure and velocity was conducted by PISO algorithm. The energy balance equation was incorporated for explicit calculation of the moving melting front location. At each interval, the buoyant convection in the melted liquid site and the conduction in the solid area were solved implicitly by a line-iteration scheme. Continuous reiterative computations were maintained to satisfy a relative convergence criterion of 10^{-6} for the whole field variables of the problem. The computational domain was discretized by 107600 quadrilateral 2D elements in which an element size was 3.75×10^{-6} m^2. A time step of 0.01 second was found to keep the required solution accuracy at a relatively low run time.

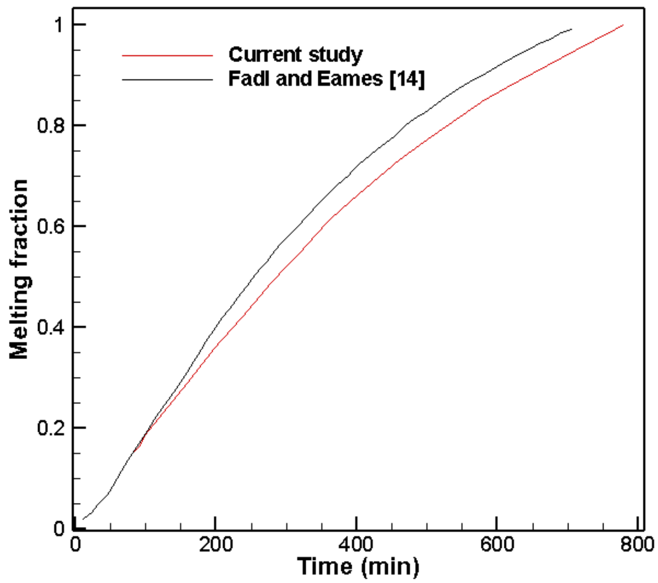

Fig. 2: Comparison between Fadl and Eames [17] as well as current simulation.

5. Results and Discussion

Due to the difference in density and heat diffusion, the amount of melting of OA in various times can be observed in Fig. 3 that it illustrates the melting fraction contours of this scenario at different times.

When OA volume ratio was 50%, first, the temperature of regions near the constant-heat flux wall started to increase. After melting of OA near the hot wall, there was a displacement between these materials due to higher density of water with respect to OA. Then, as the contact of water and solid OA near the hot wall started, the upper water continued warming and solid OA experienced slow melting, because of the lower temperature of water than the melting temperature of OA at this moment and the temperature gradients existing in the enclosure. After a large portion of the water was warmed, OA melted more quickly due to the water temperature rise and the rotational flows in water resulting from the buoyancy force. The results of melting process for OA in presence of water with the boundary condition of a constant-heat flux wall (Fig. 3) had the same melting process with the numerical results of OA in presence of water with a two-dimensional rectangular enclosure with constant temperature boundary condition obtained by Khademi et al. [18-20].

The amount of thermal flux entering the enclosure was calculated based on the temperature drop of the air as high as 1 degree of centigrade through the cavity. In this method, the amount of energy was stored faster in PCM in presence of an auxiliary fluid compared to the state that the same amount of PCM was employed without an auxiliary fluid. Also, because the heavier material was placed on top of the lighter material, their density difference caused the displacement of the two materials during the melting process, which was an extension of the acceleration of the PCM melting process. Therefore, by reducing the temperature of the intake air to the compressor, the Brayton cycle efficiency and amount of energy storage increased. Since the materials employed in this system were not soluble in each other, both materials separated at the end of the charging process, and they could be used in repeatable cycles. The materials were completely replaced by each other at the end of the melting process. Therefore, to use the system again after de-charging, it must have the ability to rotate around the horizontal axis. Also, temperature distribution of 2 specified points are shown in Fig. 4.

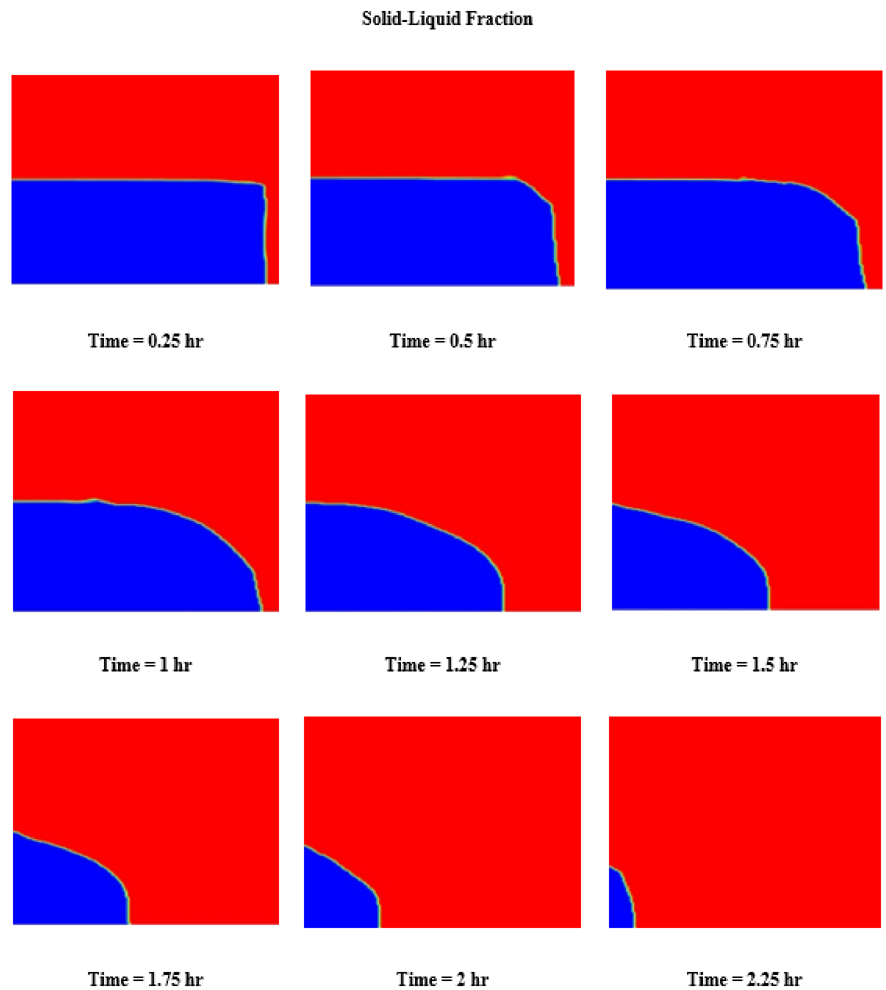

Fig. 3: Volume fractions of melting process of OA in various times.

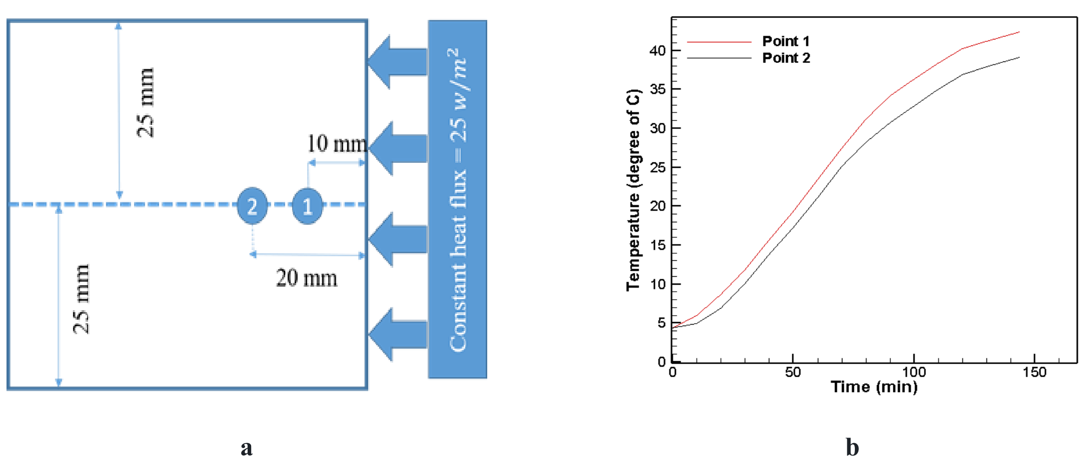

Fig. 4: (a) Schematic of 2D enclosure, and (b) temperature variation versus time at 2 points.

6. Conclusion

The present study addresses the thermodynamic efficiency improvement of a Brayton cycle power plant with a PCM based heat exchanger to cool the intake air for improving the net power output and thermal effectiveness of the plant. Further discussions include outcomes of the numerical modeling of PCM melting because of air rejecting heat to the PCM. According to PCM melting, the geometry with intake air conducted with enclosure is superior among the examined geometries in terms of heat transfer for rejection of the hotness of intake air. Around 90% of the melting occurs within almost 2.4 hours. If the intake air temperature is lowered by PCM enclosure, lowering the temperature of intake air to the compressor causes the efficiency of the Brayton cycle to increase. This valuable increase in the thermal efficiency and net power output of the Brayton cycle demonstrates the high potential of a simple PCM system. Additional detailed analyses are necessary with regard to PCM heat exchanger design, economics, and investigation for implementation of this new system in the Brayton cycle in future studies.

Acknowledgements

We would like to thank Mr. Kyle Shank from Gannon University for his kind help during the writing of manuscript.

References

[1] M. Alhazmy and Y. S. Najjar, "Augmentation of gas turbine performance using air coolers," *Applied thermal engineering,* vol. 24, no. 2-3, pp. 415-429, 2004, doi: 10.1016/j.applthermaleng.2003.09.006.
[2] M. M. Alhazmy, R. K. Jassim, and G. M. Zaki, "Performance enhancement of gas turbines by inlet air-cooling in hot and humid climates," *International journal of energy research,* vol. 30, no. 10, pp. 777-797, 2006, doi: 10.1002/er.1184.
[3] M. Ameri, H. Shahbazian, and M. Nabizadeh, "Comparison of evaporative inlet air cooling systems to enhance the gas turbine generated power," *International journal of energy research,* vol. 31, no. 15, pp. 1483-1503, 2007, doi: 10.1002/er.1315.
[4] M. Ameri, S. H. Hejazi, and K. Montaser, "Performance and economic of the thermal energy storage systems to enhance the peaking capacity of the gas turbines," *Applied thermal engineering,* vol. 25, no. 2-3, pp. 241-251, 2005, doi: 10.1016/j.applthermaleng.2004.05.012.
[5] E. Kakaras, A. Doukelis, A. Prelipceanu, and S. Karellas, "Inlet air cooling methods for gas turbine based power plants," 2006, doi: 10.1115/1.2131888.
[6] B. Mohanty and G. Paloso Jr, "Enhancing gas turbine performance by intake air cooling using an absorption chiller," *Heat recovery Systems and CHP,* vol. 15, no. 1, pp. 41-50, 1995, doi: 10.1016/0890-4332(95)90036-5.
[7] M. Ameri and S. Hejazi, "The study of capacity enhancement of the Chabahar gas turbine installation using an absorption chiller," *Applied thermal engineering,* vol. 24, no. 1, pp. 59-68, 2004, doi: 10.1016/S1359-4311(03)00239-4.
[8] B. Dawoud, Y. Zurigat, and J. Bortmany, "Thermodynamic assessment of power requirements and impact of different gas-turbine inlet air cooling techniques at two different locations in Oman," *Applied thermal engineering,* vol. 25, no. 11-12, pp. 1579-1598, 2005, doi: 10.1016/j.applthermaleng.2004.11.007.
[9] S. Boonnasa, P. Namprakai, and T. Muangnapoh, "Performance improvement of the combined cycle power plant by intake air cooling using an absorption chiller," *Energy,* vol. 31, no. 12, pp. 2036-2046, 2006, doi: 10.1016/j.energy.2005.09.010.
[10] V. R. Panyam and N. Banker, "Thermodynamic assessment of a gas turbine power plant integrated with an adsorption refrigeration system," *Applied Thermal Engineering,* vol. 117, pp. 577-583, 2017, doi: 10.1016/j.applthermaleng.2017.02.034.
[11] A. Brent, V. R. Voller, and K. Reid, "Enthalpy-porosity technique for modeling convection-diffusion phase change: application to the melting of a pure metal," *Numerical Heat Transfer, Part A Applications,* vol. 13, no. 3, pp. 297-318, 1988, doi: 10.1080/10407788808913615.

[12] M. Ishii and T. Hibiki, *Thermo-fluid dynamics of two-phase flow*. Springer Science & Business Media, 2010.
[13] A. Favakeh, A. Khademi, and M. B. Shafii, "Experimental Study of Double Solid Phase Change Material in a Cavity," in *ASHRAE Topical Conference Proceedings*, 2019: American Society of Heating, Refrigeration and Air Conditioning Engineers, Inc., pp. 24-31.
[14] A. Khademi, A. Mousemi, A. Parcheforosh, M. B. Shafii, and G. Sorrentino, "Simulation of Phase Change Material Melting Process in Presence of Nanofluid as an Auxiliary Fluid," in *Proceedings of the 4th International Conference on Energy Harvesting, Storage, and Transfer (EHST'20)*, 2020, doi: 10.11159/ehst20.111.
[15] A. Favakeh, A. Khademi, and M. B. Shafii, "Experimental Investigation of the Melting Process of Immiscible Binary Phase Change Materials," *Heat Transfer Engineering,* pp. 1-21, 2022, doi: 10.1080/01457632.2022.2034085.
[16] A. Khademi, A. Favakeh, M. Darbandi, and M. B. Shafii, "Numerical and Experimental Study of Phase Change Material Melting Process in an Intermediate Fluid," in *ASHRAE Topical Conference Proceedings*, 2019: American Society of Heating, Refrigeration and Air Conditioning Engineers, Inc., pp. 16-23.
[17] M. Fadl and P. Eames, "A numerical investigation into the heat transfer and melting process of lauric acid in a rectangular enclosure with three values of wall heat flux," *Energy Procedia,* vol. 158, pp. 4502-4509, 2019, doi: 10.1016/j.egypro.2019.01.761.
[18] A. Khademi, M. Darbandi, M. B. Shafii, and G. E. Schneider, "Numerical Simulation of Phase Change Materials to Predict the Energy Storage Process Accurately," in *AIAA Propulsion and Energy 2019 Forum*, 2019, p. 4225, doi: 10.2514/6.2019-4225.
[19] A. Khademi, M. Darbandi, and G. E. Schneider, "Numerical Study to Optimize the Melting Process of Phase Change Material Coupled with Extra Fluid," in *AIAA Scitech 2020 Forum*, 2020, p. 1932, doi: 10.2514/6.2020-1932.
[20] S. A. A. Mehrjardi, A. Khademi, S. Ushak, and S. Alotaibi, "Melting process of various phase change materials in presence of auxiliary fluid with sinusoidal wall temperature," *Journal of Energy Storage,* vol. 52, p. 104779, 2022, doi: 10.1016/j.est.2022.104779.